ANNALS OF WEST UNIVERSITY OF
TIMISOARA PHYSICS
Vol. LXVI, 2024

DOI: 10.2478/awutp-2024-0006

EFFECT OF RAPID THERMAL ANNEALING ON CuO NANOPARTICLES

Maria Nor Elyakin Boumezrag, Kenza Almi, Said Lakel *, Noor El Imane Zaghoum, Hanna Touhami

Laboratory of Metallic and Semiconducting Materials, University of Biskra, Algeria
**E-mail: s.lakel@univ-biskra.dz*

Article Info

Received: 24.12.2023
Accepted: 19.03.2024

Keywords:
Annealing methods, copper oxide, nanoparticles, nanoparticle synthesis methods, rapid thermal annealing

Abstract

This work is a comparative study of the effect of two different annealing methods on copper oxide (CuO) nanoparticle properties obtained previously by direct precipitation method. The prepared samples were annealed in air at various temperatures (300, 400, 500°C) for 1 hour. Then they were characterized by employing scanning electron microscopy (SEM), X-ray diffraction (XRD), UV-Visible, and Fourier Transform Infrared (FT-IR) spectroscopy. The main results revealed an increase in the grain size in both methods as the annealing temperature increases. It reaches 30.93 nm in RTA and 26.75 nm in STA at 500°C. XRD spectra showed, in the case of RTA at 500 °C, a significant decrease in the intensity corresponding to the (002) and (111) orientations. This result indicated that beyond 400 °C, one hour of RTA is not suitable for enhancing CuO nanoparticle crystallinity compared to STA. The optical analysis demonstrated that the energy of the optical band gap in STA is higher than that in RTA. It reaches 2,88 eV at 500°C using RTA which is close to the gap value of CuO in the range of 1.8–2.8 eV. FT-IR results showed, for both methods, the presence of characteristic peaks of the Cu-O bonds in the monoclinic CuO structure without any trace of Cu_2O structure. Nevertheless, samples exposed to RTA for one hour are more susceptible to absorbing species of C=O bond (C=O bond is due to the atmospheric CO_2 absorption and the presence of organic impurities from the synthesis process) than those of STA. Hence, RTA at 500 °C is far from producing CuO nanoparticles with preferred characteristics; it needs further research to examine the effect of higher temperature by controlling the annealing time.

1. Introduction

Among metal oxides, nanoparticles have gained importance due to their very different properties compared to those of bulk material [1]. Their properties depend on their size, shape, and morphology [2-4]. Thus, the main advantage of nanomaterials is that they can be used to improve current materials or create new ones with exceptional properties.

Due to its outstanding properties, cooper oxide nanostructures attract considerable attention. Cooper oxide is non-toxic , its constituents are available in abundance, it is a good solar light absorber [5], a good electrical conductor [6], and it is stable at high pressure and temperature [7]. The enhancement in these properties can be influenced by the morphology of its nanostructures which in turn depends on the process of synthesis [3, 6, 8, 9].

The thermal annealing process is an important step in synthesizing nanostructures of metal oxides including copper oxide. There are two techniques of thermal annealing which include slow thermal annealing (STA) and rapid thermal annealing (RTA). The influence of annealing process on thin film cooper oxide nanostructures is most commonly studied by researchers [10-15] due to the possible multiple applications of these kind of materials [6, 16, 17]. Some of them confirmed the efficient impact of STA in an optimum annealing temperature range of 200-650°C on structural and electrical properties of copper oxides thin films [10-12, 18-22], while others demonstrated that RTA is an effective and efficient technique to enhance the structural properties with the aid of high annealing temperature ranging from 400°C to 800°C at different duration in accordance to the used temperature [13-15, 23].

Although several studies showed the effective implementation of cooper oxide nanoparticles and their importance in environmental, energetic [24-33], and therapeutical purposes, annealing process represents a crucial step in production of such materials. However, there are only few reports describing the effects of annealing temperature referring to cooper oxide nanoparticles [24, 40, 41].

Yet, in all previous research, the annealing process was performed in different experimental conditions which in turn influence the obtained results. No study was conducted so far that reported the results of the effect of a rapid and slow thermal annealing process performed under the same experimental conditions to conclude the efficiency of one annealing method relative to the other. Therefore, the aim of this work is to examine the efficiency of rapid annealing and its effect on the physical properties of cooper oxide nanoparticles in comparison to the slow annealing process.

2. Materials and Methods

2.1. CuO nanoparticles synthesis

CuO nanoparticles were synthesized using the precipitation method through the following process: 2 g of $CuSO_4.5H_2O$ is dissolved in 20 ml of distilled water. In addition, 8 g of NaOH has been dissolved in 200 ml of the same solvent. Each solution is stirred separately for a few minutes at room temperature to obtain two homogenous solutions of 0.4 mol/l and 1

mol/l respectively. Sodium hydroxide solution is completely added to the first solution of cupric sulfate and then stirred for one hour on a heating plate set at 100 °C. The solution is then left to cool at room temperature followed by filtration process to get a black powder. The filtered material is carefully collected and dried in an oven for an hour at 100 °C to evaporate all residual solvents on the substrate surface. After that, it was milled using a ceramic mortar, which resulted in cooper oxide nano sized particles.

2.2. Specimen preparation

After synthesizing CuO nanoparticles, they were divided into two portions. From the first portion, three fractions were prepared to undergo a rapid heat annealing at 300 °C, 400 °C, and 500 °C for one hour. In the same way, three other fractions were prepared from the second portion but this time they undergo a slow heat annealing at the same temperatures and during the same time. In both annealing processes, a Nabertherm GmbH annealing furnace was used. It is an electrically heated furnace that heats from 30 to 3000 °C.

In STA, the sample is heated gradually in the oven starting from room temperature to the target temperature with a heating rate of 2 °C per minute. Once the set temperature is reached, the heating is maintained constant for one hour when it automatically stops heating allowing gradual cooling of the sample. Whereas in the case of the RTA, the sample is heated directly at the desired temperature for one hour, then it is immediately removed from the oven and cooled at room temperature. Afterwards, the sample is put in a special glass tube which is brought in through a hole drilled in the back of the oven made to evacuate the vapour produced during heating.

After the heat treatment, different specimens were subdivided into small amounts to be characterized.

2.3. Specimen characterization

To determine the nanoparticles' size and shape, a morphological study was conducted using a Scanning Electron Microscope type TESCAN-VEG03. Magnification of 5 µm has been used. Structural properties were studied using Rigaku Mini Flax 600 X-ray diffractometer (Cu Kα radiation, λ = 1,54056 A°), X-ray diffraction patterns were set between $2\theta = 20°$ and 80° with a step of 0.5° per minute. In addition, infrared spectrophotometry (FT-IR-8400S) was used as well. Optical properties were analyzed employing a UV-Visible spectrophotometer (PerkinElmer-Lambda 25), the spectral range was measured between 200 and 800 nm.

3. Results and discussion

3.1. Morphological Analysis

SEM images of the surface morphology of the prepared CuO nanoparticles are presented in Figure 1. They show that most CuO nanoparticles are sheet-like shaped. Similar morphology was found in the literature using the same synthesizing method [41]. Since the sheet average particle size varies in a broad range it is not practical nor easy to determine the exact particle size of the sample. Nevertheless, SEM results reveal some distinctions between the morphology of RTA and STA samples annealed at different temperatures. RTA images at different temperatures show an inhomogeneous distribution of the nanoparticles with large conglomerates compared to STA samples [10]. This could be justified by the grain growth mechanism correlated to rapid thermal annealing [42, 43]. The fast ramping to the target temperature triggers the nucleation process within a short time, a higher temperature generates high pressure which promotes the mutual diffusion of small and intermediate grains during annealing, resulting in larger agglomerates [10, 44].

3.2. Structural Analysis

The X-ray diffractograms of the prepared CuO nanoparticles are presented in Figure 2. The results show that the peaks in all obtained XRD spectra are well-matched with the monoclinic phase of CuO crystals (JCPDS card No. 080-1268). All samples exhibit the same preferential orientations, (111) and (002) which agree with research on copper oxide nanoparticles [8, 9]. X-ray diffractogram analysis demonstrates that in both methods the diffracted intensity of the most intense peaks increases with the increase of the temperature except for the case of RTA at 500°C, where it decreases significantly as depicted in Figure 3 a, b. It is also noticeable that STA's peaks are more intense than RTA's peaks at all positions and almost at all the studied annealing temperatures (Figure 2). Further, Table 1 indicates that the crystallite size calculated in both techniques of annealing increases with the increase of the temperature but it takes higher values in RTA's cases.

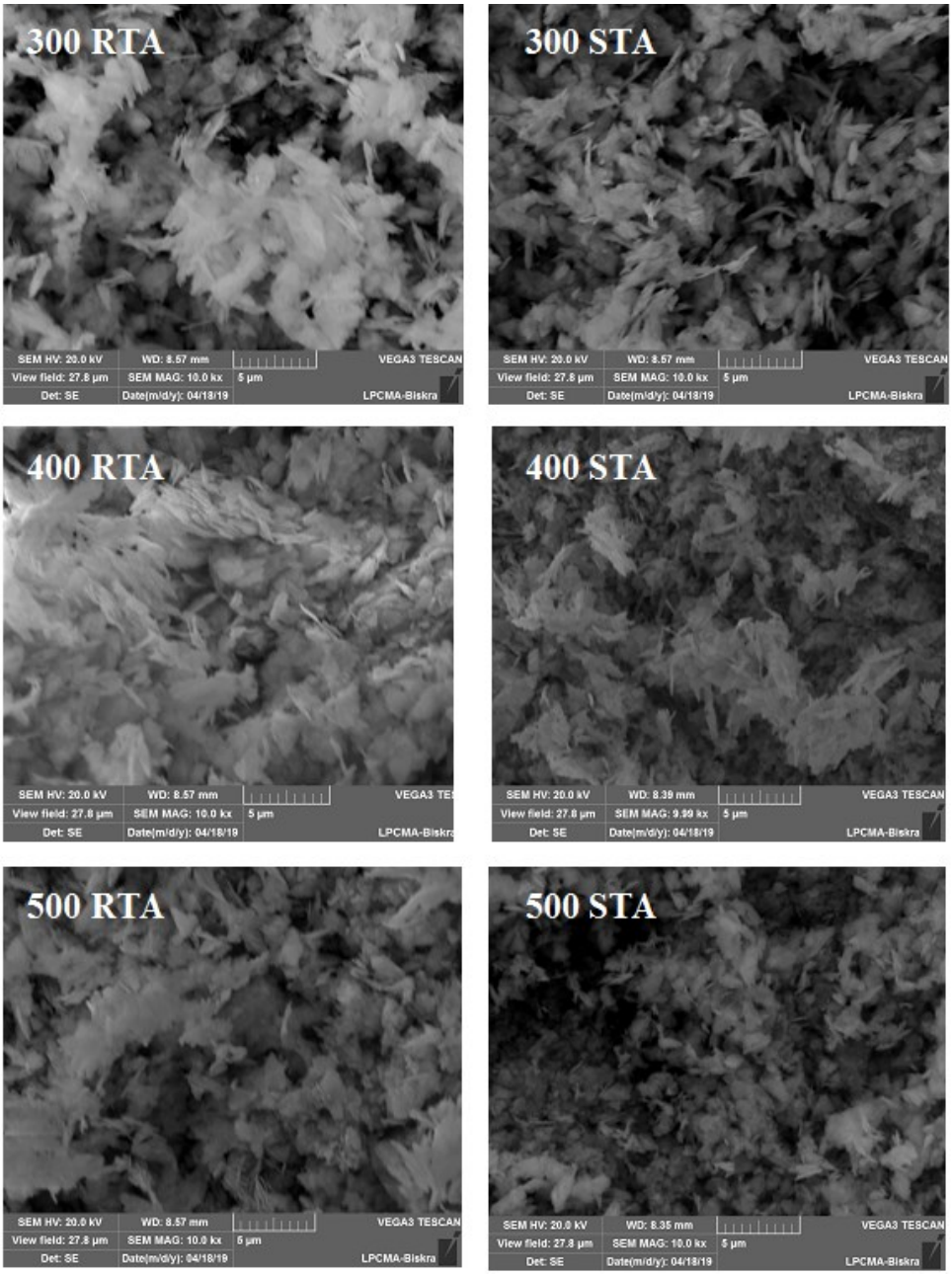


Figure 1. SEM images of the CuO nanoparticles synthesized using (a) RTA and (b) STA at 300°C, 400°C, and 500°C for one hour of annealing.

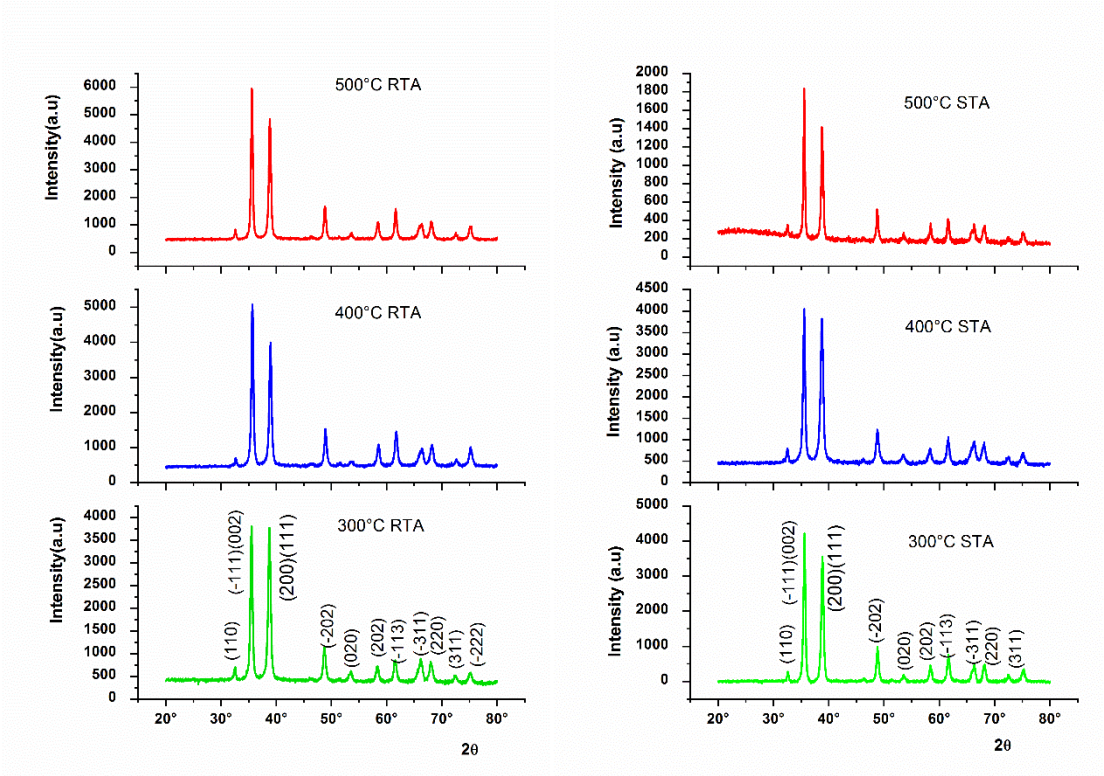


Figure 2. XRD patterns of CuO nanoparticles prepared with RTA and STA at 300°C, 400°C, 500°C for one hour of annealing

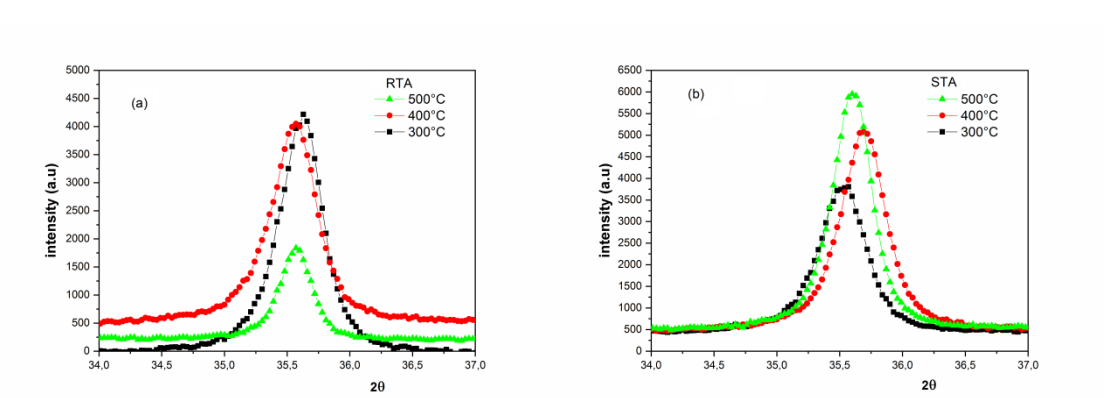


Figure 3. The predominant peak corresponding to the (002) orientation as a function of annealing temperature and method: (a) RTA case, (b) STA case

To explain those observations, it is necessary to return to the factors associated with both peak intensity and crystallite size. Thermal treatment increases the crystalline nature which leads to an increase in the number of grains orientated in a particular direction. By increasing the annealing temperature, many different grains of the same orientation coalesce together and form a large grain having a certain orientation. Therefore, the diffracted intensity is supposed to be increased as the crystallite size increases which is the case with STA samples. In contrast,

RTA's spectrum measured at 500 °C revealed a significant decrease in the intensity even though the crystallite size increased at that temperature. This proves that texture may change during grain growth and affects the kinetics in the process of rapid annealing [45].

This could be justified by the fact that the rapid annealing process at high temperature (above 400 °C) for one hour can favor the crystallization process but at the same time may produce microcracks in the growing grains after sudden cooling from high temperature to room temperature [46, 47]. These micro-cracks can scatter X-rays in different directions thereby changing the texture and reducing the peak intensity in a particular direction as indicated in Figure 3a. As it can be attributed to the grain recrystallization in contrast to recovery behavior which occurs in the case of RTA at relatively high temperatures [46, 47]. recrystallization results in the formation of new grain orientations which explains the reduction of the peak intensity and the recovery occurs during the incubation period for recrystallization [47], which, on the other hand, explains why the grain size did not decrease. Peak intensity can increase again when the recrystallization is completed and this depends on both the annealing time and temperature [45-49].

For this reason, further study is required to be conducted about the effect of rapid thermal annealing time and temperature.

The high intensity of STA's peaks compared to RTA's peaks may be explained by the difference in the crystal structure factor of the samples. The intensity diffracted in a specific orientation is directly related to the square of the structure factor modulus. This latter indicates the overall ray diffusion from every crystal plane and depends on the arrangement of atoms in the crystal. In other words, it is related to both the crystal structure and composition. Therefore, the peak intensity is affected by the thermal agitation of the atoms and, broadly, by the disorder. Atoms which have treated by rapid heating are agitated and susceptible to disorders more than those undergone slow heating. The latter has time to return to its equilibrium state, this leads to a low state of disorder and high diffracted intensity.

In addition, Figure 3 shows that by increasing temperature, curves shift towards increasing θ in both methods, especially in the STA method; this means that the nanoparticles have undergone compressive stress. This can be explained by the merging process induced by increasing thermal annealing and this, in turn, increases the grain size [10, 42].

In the temperature range of 300 to 500 °C, the crystalline size increases from 19.99 to 31.47 nm. Table 1 presents the calculated compressive stress and dislocation density (δ) values. Where δ is obtained from the crystallite size (D), according to the formula [50]:

$$\delta = \frac{1}{D^2} \quad (1)$$

Whereas, the micro stain values were determined using the following formula [50]

$$\varepsilon = \frac{\beta \cos\theta}{4} \quad (2)$$

As illustrated in Table 1, the dislocation density and the compressive stress values decrease as the temperature increases in both techniques of annealing. The decrease is slightly higher in RTA than in STA. The increase in the temperature increases the kinetics and the interactions of the dislocations. This leads to an increase in the migration and annihilation of the dislocation and consequently to a decrease in their density.

Table 1. Structural properties of CuO nanoparticles annealed following two methods

Annealing Method	STA			RTA		
Annealing temperature T(°C)	300	400	500	300	400	500
Cristillize size (nm)	22.28	23.48	26.75	22.36	24.22	30.93
Strainε (%) 10^{-2}	0.146	0.141	0.120	0.139	0.133	0.099
Dislocation density σ (nm^{-2}) 10^{-2}	0.201	0.181	0.139	0.200	0.170	0.104

However, rapid thermal annealing enhances the concentration of the vacancies in the lattice arrangement which, in turn, increases the velocity of dislocation glide motion. Therefore, the dislocation density is reduced more effectively in rapid thermal annealing than in slow thermal annealing. This can also be attributed to the grain boundary effects. It is known that dislocation density, stress, and grain boundary size are interrelated [51]; Grain boundaries play an important role in strain-hardening. They prevent dislocations from moving in the metal while it is being strained. The more dislocations are blocked; it becomes harder for the metal to deform. That's probably what happened in the case of the RTA in which crystallite size takes higher values than those in STA; thereby, higher values of boundary size and lower values of stress.

3.3. Optical analysis

The optical band gap energy (Eg) of CuO nanoparticles was estimated employing the absorption spectrum fitting method (ASF) [52]. In this method, the optical band gap can be calculated using only the absorbance spectrum without any need for calculating the thickness. It is based on the following equation [52]:

$$A = B_1\lambda(\frac{1}{\lambda} - \frac{1}{\lambda_g})^m + B_2 \quad (3)$$

Where A is the absorbance, λ is the wavelength, B_1 and B_2 are independent of λ, m takes the value of $\frac{1}{2}$ for the best fitting.

Thus the value of the band gap is obtained from $\frac{1}{\lambda_g}$, where Eg equal to $\frac{1240}{\lambda_g}$. The value of λ_g can be determined by extrapolating the straight line of $(\frac{A}{\lambda})^2$ versus $\frac{1}{\lambda}$ curves, shown in Figure 4, at $(\frac{A}{\lambda})^2 = 0$. Table 2 displays the variation in the optical gap as a function of the annealing temperature. It can be noticed that the optical gap decreased by increasing the annealing temperature in the two cases of the annealing method. However, the RTA method yielded lower values of the energy gap, especially at 500 °C (Figure 5). This may be justified by the fact that the increase in particle size decreases the optical gap according to the potential well quantum theory, i.e the quantum confinement in nanometer particle-sized materials. This result confirms what is mentioned above (Figure 1): the particle size of RTA is larger than the particle size of STA.

Table 2. Energy gap values calculated using two methods of annealing at different temperatures

AnnealingTemperatureT(°C)	300	400	500
RTA : Eg (eV)	3.72	3.63	2.88
STA : Eg (eV)	3.91	3.87	3.79

On the other hand, to better understand the effect of two types of annealing processes on the structure of copper oxide, an infrared absorption bands analysis was performed. FT-IR spectra of all the samples are presented in Figure 6. All samples' spectra show a wide band located at around ~ 3440 cm^{-1} corresponding to the O-H group stretching of a water molecule adsorbed on the oxide surface [53], and an intense peak located at ~ 1384 cm^{-1} which is attributed to the stretching vibration of C=O group, indicating the presence of absorbed species in the surface of nanoparticles [53, 54]. CuO is a compound composed of copper and oxygen atoms. It's an inorganic compound; typically it should not contain carbon-oxygen bonds within its structure. However, a peak at 1384 corresponds to a C-O bond (by comparison to the standard chemical tables of chemical element bonds) appears in the FTIR spectrum of CuO nanopowder. We justify that the presence of organic impurities from the synthesis process especially at the level of the oven (heat treatment) since we have used atmosphere annealing

for our samples not under a vacuum annealing process (1384 cm^{-1} peak is due to the atmospheric CO_2 absorption). This problem is commonly noticed when analyzing FTIR spectra of many inorganic materials and the atmospheric CO_2 absorption; it's considered as sources of contamination or interference that lead to unexpected signals. Another intense peak at around 613 cm^{-1} is attributed to the Cu-OH vibration bands [54], but the most intense absorption band is located at around 494 cm^{-1} and 504 cm^{-1}, it is assigned to the stretching vibrations of Cu-O indicating the formation of copper oxide [55]. It is noticed that by increasing the annealing temperature, Cu-O bond concentration increased and Cu-OH bond concentration decreased especially in the case of RTA. However, the decrease of O-H and C=O bond concentration is noticed in the case of STA, particularly at 500°C where the O-H group disappears. This means that 500 °C is not sufficient to remove all residues and impurities in RTA more than in STA. No FT-IR peak of Cu_2O existed in all synthesized samples. Both methods of annealing did not affect the crystal phase of CuO nanoparticles but affected only the crystal quality. The same result was found in the literatures [41, 56].

On the other hand, to better understand the effect of two types of annealing processes on the structure of copper oxide, an infrared absorption bands analysis was performed. FT-IR spectra of all the samples are presented in Figure 6. All samples' spectra show a wide band located at around ~ 3440 cm^{-1} corresponding to the O-H group stretching of a water molecule adsorbed on the oxide surface [53], and an intense peak located at ~ 1384 cm^{-1} which is attributed to the stretching vibration of C=O group, indicating the presence of absorbed species in the surface of nanoparticles [53, 54]. CuO is a compound composed of copper and oxygen atoms. It's an inorganic compound; typically, it should not contain carbon-oxygen bonds within its structure. However, a peak at 1384 corresponds to a C-O bond (by comparison to the standard chemical tables of chemical element bonds) appears in the FTIR spectrum of CuO nanopowder. We justify that the presence of organic impurities from the synthesis process especially at the level of the oven (heat treatment) since we have used atmosphere annealing for our samples not under a vacuum annealing process (1384 cm^{-1} peak is due to the atmospheric CO_2 absorption). This problem is commonly noticed when analyzing FTIR spectra of many inorganic materials and the atmospheric CO_2 absorption; it's considered as sources of contamination or interference that lead to unexpected signals. Another intense peak at around 613 cm^{-1} is attributed to the Cu-OH vibration bands [54], but the most intense absorption band is located at around 494 cm^{-1} and 504 cm^{-1}, it is assigned to the stretching vibrations of Cu-O indicating the formation of copper oxide [55]. It is noticed that by increasing the annealing temperature, Cu-O bond concentration increased and Cu-OH bond concentration decreased

especially in the case of RTA. However, the decrease of O-H and C=O bond concentration is noticed in the case of STA, particularly at 500°C where the O-H group disappears. This means that 500 °C is not sufficient to remove all residues and impurities in RTA more than in STA. No FT-IR peak of Cu_2O existed in all synthesized samples. Both methods of annealing did not affect the crystal phase of CuO nanoparticles but affected only the crystal quality. The same result was found in the literatures [41, 56].

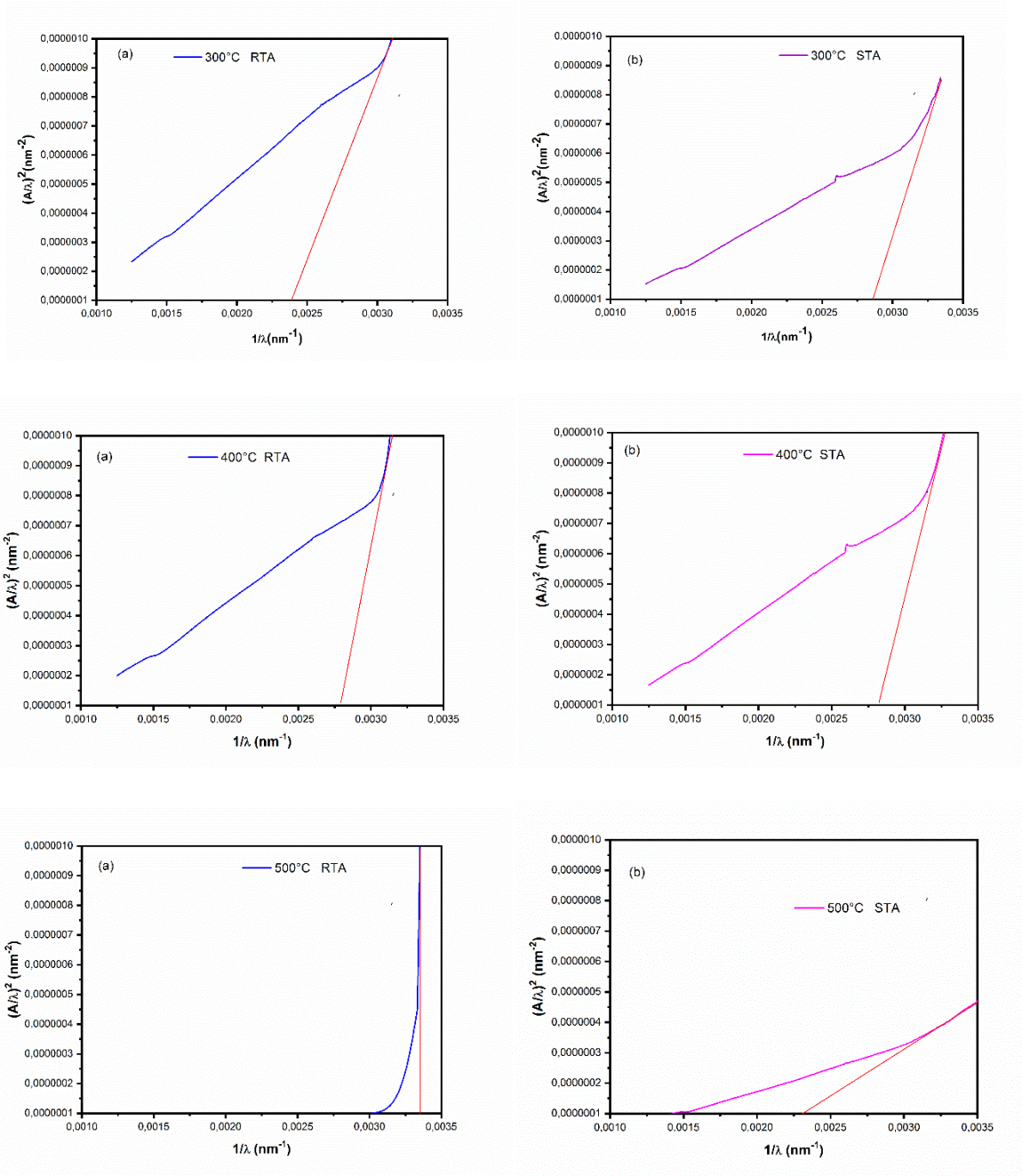


Figure 4. ASF diagrams for samples prepared using (a) RTA and (b) STA annealing methods at 300°C, 400°C and 500°C for one hour of annealing

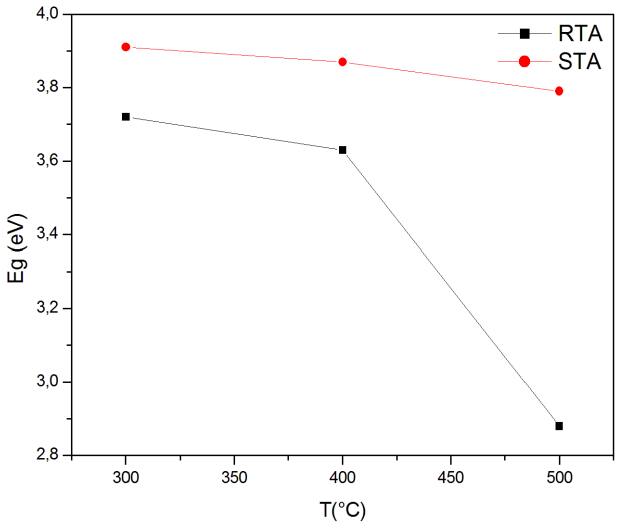
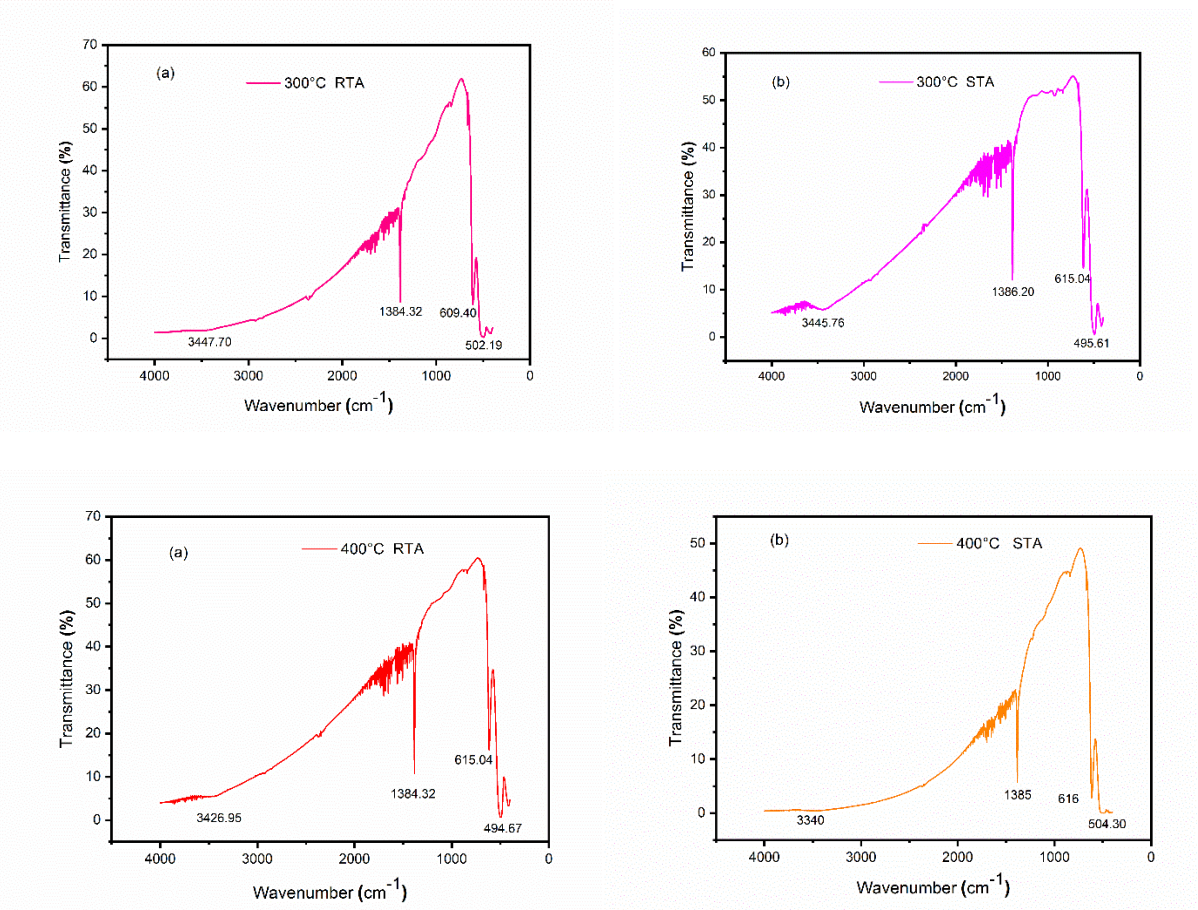


Figure 5. Optical band gap energy of the prepared CuO nanoparticles as a function of annealing temperature following two methods: RTA and STA for one hour of annealing



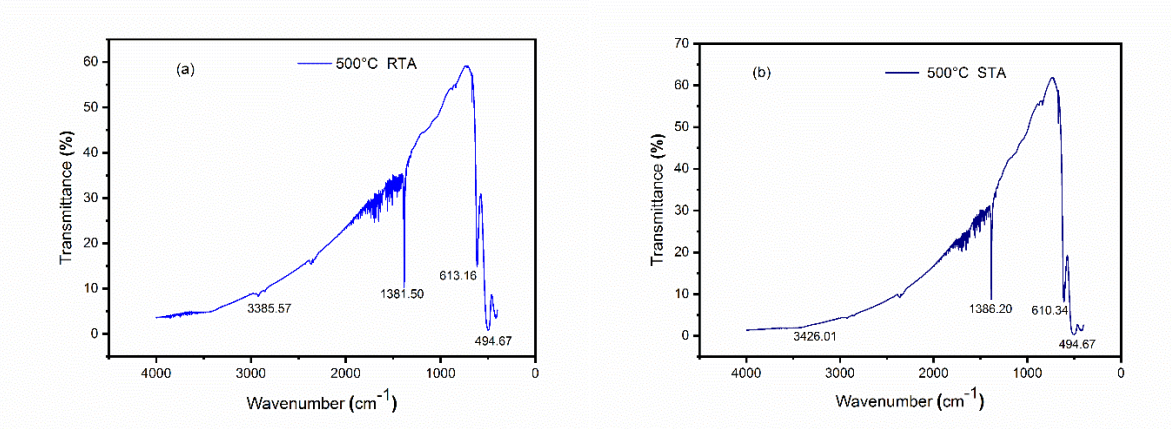


Figure 6. FTIR spectra of CuO nanoparticles prepared following: (a) RTA and (b) STA at 300°C, 400°C, 500°C for one hour

4. Conclusions

In summary, this work reports the results of rapid and slow temperature annealing effect on the structural and optical properties of copper oxide nanoparticles. RTA and STA effect was studied for the first time under the same working conditions using the direct precipitation method to synthesize copper oxide nanoparticles. The objective of this work is to provide data on the effect of rapid thermal annealing on copper oxide nanoparticle properties and to examine its efficiency compared to slow thermal annealing in enhancing these properties. The results showed that samples in both methods exhibit a sheet-like shape at different tested temperatures. They revealed a change in the texture of samples that underwent rapid thermal annealing at 500 °C for 1 hour. Compared to STA, RTA at 500 °C is not sufficient to remove all residues and impurities but it recorded relatively the lowest value of band gap energy. Thus, rapid thermal annealing at 500°C resulted in improved optical properties of CuO nanoparticles whereas STA resulted in improved crystalline nature of CuO nanoparticles. Further increases in annealing temperature and reductions in annealing time at the target temperature are needed to study the effect of RTA on improving the crystallinity of copper oxide nanoparticles.

References

[1]Khan, I., Saeed, K., & Khan, I. *Nanoparticles: Properties, applications and toxicities,* Arabian Journal of Chemistry (2017) doi:10.1016/j.arabjc.2017.05.011

[2]Rehman, S., Mumtaz, A., & Hasanain, S. K., *Size effects on the magnetic and optical properties of CuO nanoparticles,* Journal of Nanoparticle Research, 13(6), (2010) 2497–2507, doi:10.1007/ s11051-010-0143-8

[3] Neeleshwar, S., Chen, C. L., Tsai, C. B., Chen, Y.Y, Chen, C.C., Shyu, S. G., Seehra, M.S., *Size-dependent properties of CdSe quantum dots.* Physical Review B, 71(20), (2005) 201307R doi:10.1103/physrevb.71.201307

[4] Anandan, S., Lee, G. J., & Wu, J. J. *Sonochemical synthesis of CuO nanostructures with different morphology.* Ultrasonics Sonochemistry*, 19(3), 682–686*(2012) doi:10.1016/j.ultsonch.2011.08.0

[5]Yu. P. Sukhorukov*, B. A. Gizhevskii, E. V. Mostovshchikova, A. Ye. Yermakov, S. N. Tugushev, and E. A. Kozlov, *Nano-crystalline copper oxide for selective solar energy absorbers,* Tech. Phys. Lett. *32, 132* (2006)

[6]Zhang, H., & Zhang, M., *Synthesis of CuO nanocrystalline and their application as electrode materials for capacitors,* Materials Chemistry and Physics*, 108(2-3),* (2008) *184–187.* doi:10.1016/ j.matchemphys.2007.10

[7]Devi, H.S., Singh, T.D., *Synthesis of copper oxide nanoparticles by a novel method and its application in the degradation of methyl orange.* Adv. Electr. Comput. Eng.*4(1)* (2014) *83–8*.

[8]Zhu, J., Li, D., Chen, H., X Yang, L Lu, X Wang*, Highly dispersed CuO nanoparticles prepared by a novel quick-precipitation method.* Materials Letters, *58(26),* (2004) *3324–3327.* doi:10.1016/j.matlet.2004.06.031

[9]Mallick, P., Sahu, S., *Structure, Microstructure and Optical Absorption Analysis of CuO Nanoparticles Synthesized by Sol-Gel Route*. J. Nanosci. Nanotechnol*. 2(3), (2012) 71-74.* DOI: 10.5923/j.nn.20120203.05

[10] Touka, N., Tabli, D., Badari, K., *Effect of annealing temperature on structural and optical properties of copper oxide thin films deposited by sol-gel spin coating method***,** Journal Of Optoelectronics And Advanced Materials, 21 (11-12) (2019) 698 – 701

[11] Raship, N. A., Sahdan, M. Z., Adriyanto, F., Nurfazliana, M. F., Bakri, A. S, *Effect of annealing temperature on the properties of copper oxide films prepared by dip coating technique* (2017). doi:10.1063/1.4968374

[12] Serin, N., Serin, T., Horzum, Ş., & Çelik, Y, *Annealing effects on the properties of copper oxide thin films prepared by chemical deposition.* Semiconductor Science and Technology, 20(5), (2005) 398–401. doi:10.1088/0268-1242/20/5/012

[13] Masudy-Panah, S., Moakhar, R. S., Chua, C. S., Kushwaha, A., Wong, T. I. and Dalapati, G. K., *Rapid thermal annealing assisted stability and efficiency enhancement in a sputter deposited CuO photocathode.* RSC Advances, 6(35), 29383–29390 (2016) doi:10.1039/c6ra03383k

[14] Gottesman, R., Song, A., Levine, I., Krause, M., Islam, A. N., Abou-Ras, D., Dittrich, T., Van de Krol, R. and Chemseddine, A., *Pure CuBi2 O4 Photoelectrodes with Increased Stability by Rapid Thermal Processing of Bi2 O3 /CuO Grown by Pulsed Laser Deposition.* Advanced Functional Materials*, 1910832 (2020)*

[15] Bergum, K., Riise, H. N., Gorantla, S., Krause, M., Islam, A. N., Abou-Ras, D., Dittrich, T., Van de Krol, R. and Chemseddine, A, *Improving carrier transport in Cu2O thin films by rapid thermal annealing.* Journal of Physics: Condensed Matter, 30(7) (2018), 075702. doi:10.1088/1361-648x/aaa5f4

[16] Vasiliev, R. B., Rumyantseva, M. N., Gaskov. A. M. (1998). *CuO/SnO2 thin film etero structures as chemical sensors to H_2S.* Sensor Actuat B. 50, 186-193.

[17] Ishihara, T., Higuchi, M., Takagi, T., Ito, M., Nishiguchi, H., Takita, Y*., Preparation of CuO thin films on porous BaTiO3 by self-assembled multibilayer film formation and application as a CO2 sensor,* Journal of Materials Chemistry, *8(9)* (1998) *2037–2042.* doi:10.1039/a801595c

[18] Mammah, S. L., Opara, F. E., Omubo-Pepple, V. B., Joseph Effiom-Edem Ntibi, Sabastine Chukwuemeka Ezugwu, Fabian Ifeanyichukwu Ezema, *Annealing effect on the optical and solid state properties of cupric oxide thin films deposited using the Aqueous Chemical Growth (ACG) method.* Natural Science, 05 (03) (2013) 389–399 doi:10.4236/ns. 2013.53052

[19] Hashim, H., Samat, S. F. A., Shariffudin, S. S., & Saad, P. S. M. (2018). *Investigation of Annealing Temperature on Copper Oxide Thin Films Using Sol-Gel Spin Coating Technique.* IOP Conference Series: Materials Science and Engineering, 340, 012008. doi:10.1088/1757-899x/340/1/012008

[20] Wojcieszak, D., Obstarczyk, A., Mankowska, E., Mazur, M., Kaczmarek, D., Zakrzewska, K., Mazur, P., Domaradzki, J. *Thermal oxidation impact on the optoelectronic and hydrogen sensing properties of p-type copper oxide thin films.* Materials Research Bulletin, 147 (2022) 111646 doi.10.1016/j.materresbull.2021.111646

[21] Al Armouzi, N., El Hallani, G., Liba, A., Zekraoui, M., Hilal, H.S., Kouider, N., Mabrouki, M., *Effect of annealing temperature on physical characteristics of CuO films deposited by sol-gel spin coating.* Materials Research Express. (2019) 10.1088/2053-1591/ab44f3

[22] Akgul, U., Yildiz, K., & Atici, Y. (2016). *Effect of annealing temperature on morphological, structural and optical properties of nanostructured CuO thin film,* The European Physical Journal Plus, 131(4). doi:10.1140/epjp/i2016-16089-3

[23] Martínez-Saucedo, G., Torres-Delgado, G., Márquez-Marín, J., Zelaya-Ángel, O., Castanedo-Pérez, R., *Copper oxide and tin oxide amorphous-thin-film heterojunction diodes obtained via solution-based techniques with increased rectification after rapid thermal annealing treatments.* Journal of Alloys and Compounds, (2020) *157790.* doi:10.1016/j.jallcom.2020.157790

[24] Xiong, L., Xiao, H., Chen, S., Chen, Z., Yi, X., Wen, S., Zheng, G., Ding, Y., Yu, H., *Fast and simplified synthesis of cuprous oxide nanoparticles: annealing studies and photocatalytic activity.* RSC Adv., 4(107) (2014) *62115–62122.* doi:10.1039/c4ra12406e

[25] Liu, D., Zhou, W., Wu, J., *CuO-CeO2/ZSM-5 composites for reactive adsorption of hydrogen sulphide at high temperature*. Can. J. Chem. Eng. 94, (2016) 2276–2281. http://dx. doi.org/10. 1002/cjce.22613.

[26] Maini, A., & Shah, M. A., *Investigation on physical properties of nanosized copper oxide (CuO) doped with cobalt (Co): A material for electronic device application. International* Journal of Ceramic Engineering & Science. (2021) doi:10.1002/ces2.10097

[27] Gawande, M. B., Goswami, A., Felpin, F.-X., Asefa, T., Huang, X., Silva, R., Zou, X., Zboril, R., Varma, R. S., *Cu and Cu-Based Nanoparticles: Synthesis and Applications in Catalysis,* Chemical Reviews, *116(6)*(2016)*3722–3811* doi:10.1021/ acs.chemrev.5b00482

[28] Ovchinnikov, S. G., Gizhevskiĭ, B. A., Sukhorukov, Y. P., Ermakov, A. E., Uĭmin, M. A., Kozlov, E. A., Kotov, Ya. A. & Bagazeev, A. V, *Specific features of the electronic structure and optical spectra of nanoparticles with strong electron correlations. Physics of the Solid State, 49(6)* (2007) *1116–1120.* doi:10.1134/s1063783407060169

[29] Eranna, G., Joshi, B. C., Runthala, D. P., & Gupta, R. P., *Oxide Materials for Development of Integrated Gas Sensors—A Comprehensive Review.* Critical Reviews in Solid State and Materials Sciences, 29(3-4)(2004) 111–188. doi:10.1080/10408430490888977

[30] Gao, P., Chen, Y., Lv, H., Li, X., Wang, Y., Zhang, Q., *Synthesis of CuO nanoribbon arrays with noticeable electrochemical hydrogen storage ability by a simple precursor dehydration route at lower temperature*. International Journal of Hydrogen Energy*, 34(7 (2009) 3065–3069.* doi:10.1016 /j.ijhydene.2008.12.05

[31] Arbuzova, T. I., Gizhevskii, B. A., Naumov, S. V., Korolev, A.V., Arbuzov, V.L., Shal'nov, K.V., Druzhkov, A.P.,*Temporal changes in magnetic properties of high-density CuO nanoceramics.* Journal of Magnetism and Magnetic Materials, 258(2003)-259 342–344. doi:10.1016/s0304-8853(02)01052-1

[32] Gao, X. P., Bao, J. L., Pan, G. L., Zhu, H. Y., Huang, P. X., Wu, F., Song, D. Y. *Preparation and Electrochemical Performance of Polycrystalline and Single Crystalline*

CuO Nanorods as Anode Materials for Li Ion Battery. The Journal of Physical Chemistry B, 108(18) (2004) 5547–5551. doi:10.1021/jp037075k

[33] Udani, P. P. C., Gunawardana, P.V.D.S., Lee, H. C., Kim, D. H., *Steam reforming and oxidative steam reforming of methanol over CuOCeO2 catalysts,* Int. J. Hydrogen Energy 34 (2009)7648

[34] Toolabi, A., Zare, M., Rahmani, A., *Hoseinzadehd, E., Sarkhoshe, M., and Zare., M. Investigating Toxicity and Antibacterial Aspects of Nano ZnO, TiO2 and CuO with Four Bacterial Species*. J. Basic. Appl. Sci. Res. 3.2 (2013) 221-226.

[35] Jadhav, S., Gaikwad, S., Nimse, M., & Rajbhoj, A., *Copper Oxide Nanoparticles: Synthesis, Characterization and Their Antibacterial Activity.* Journal of Cluster Science, 22(2) (2011) 121–129. doi:10.1007/s10876-011-0349-7

[36] Rahim, A., Rehman, Z. U., Mir, S., Muhammad, N., Rehman, F., Nawaz, M. H., Yaqub, M., Siddiqi, S. A., Chaudhry, A. A, *A non-enzymatic glucose sensor based on CuO-nanostructure modified carbon ceramic electrode.* Journal of Molecular Liquids, 248 (2017) 425–431. doi:10.1016/j.molliq.2017.10.087

[37] Rehana, D., Mahendiran, D., Kumar, R. S., & Rahiman, A. K., *Evaluation of antioxidant and anticancer activity of copper oxide nanoparticles synthesized using medicinally important plant extracts*. Biomedicine & Pharmacotherapy, 89 (2017) 1067–1077. doi:10.1016/j.biopha.2017.02.101

[38] Akintelu, S. A., Folorunso, A. S., Folorunso, F. A., & Oyebamiji, A. K., *Green synthesis of copper oxide nanoparticles for biomedical application and environmental remediation.* Heliyon, 6(7) (2020), e04508. doi:10.1016/j.heliyon.2020.e04508

[39] Unutulmazsoy, Y., Cancellieri, C., Lin, L., Jeurgens, L. P. H., *Jeurgens, Reduction of thermally grown single-phase CuO and Cu2O thin films by in-situ time-resolved XRD,* Applied Surface Science 588 (2022)*152896*

[40] Thi, T. H., Cong1, B. T., Hai, P. N., Hoang, N., Chinh, H. V., Huong, B. T., N. T. Linh, N. T., Son, B. T., Hoa, T. T. Q., Viet, T. N., *Preparation of CuO Nanorods by Thermal Oxidation in Ozone Ambient,* VNU Journal of Science: Mathematics – Physics, Vol. 38, No. 2 (2022) 9-15

[41] Siddiqui, V. U., Ansari, A., Khan, I., Akram, M.K., Siddiqi, W.A. *Sol-gel synthesis of copper (II) oxide/alginate (CuO/Alg) bio-nanocomposite and effects of rapid thermal annealing on its properties and structure.* Materials Research Express, 6(11) (2019) 115095. doi:10.1088/2053-1591/ab4ace

[42] Khan, S. N., Ge, S., Gu, E., Karunakaran, S.K., Yang, W., Hong, R., Mai, Y., Lin, X., Yang, G., *Bifacial Cu 2 ZnSn(S,Se) 4 Thin Film Solar Cell Based on Molecular Ink and Rapid Thermal Processing.* Advanced Materials Interfaces, 8(18) (2021) 2100971. doi: 10.1002/admi.202100971

[43] Mainz, R., Walker, B. C., Schmidt, S.S., Zander, O., Weber, A., Rodriguez-Alvarez, H., Just, J., Klaus, M., Agrawal, R., Unold, T. *Real-time observation of $Cu_2ZnSn(S,Se)_4$ solar cell absorber layer formation from nanoparticle precursors.,* Phys. Chem. Chem. Phys., 15(2013) 18281

[44] Baqer, A. A., Matori, K. A., Al-Hada, N.M., Shaari, A.H., Kamari, H.M., Saion, E., Chyi, J.L.Y., Azurahanim Abdullah, C, *Synthesis and characterization of binary (CuO)0.6 (CeO2)0.4 nanoparticles via a simple heat treatment method.* Results in Physics, 9 (2018) 471–478. doi:10. 1016 /j.rinp.2018.02.079

[45] Rollett, A., Humphreys, F. J., Rohrer, G. S., & Hatherly, H. *Recrystallization-and Related Annealing Phenomena ,* Elsevier, *2*(2004)*658*

[46] Lee, Y.C., Hu, S.Y., Water, W., Tiong, K.K., Feng, Z.C., Chen, Y.T., Huang, J.C., Lee, J.W., Huang, C.C., Shen, J. L., Cheng, M.H, *Rapid thermal annealing effects on the structural and optical properties of ZnO films deposited on Si substrates.* Journal of Luminescence, 129(2) (2009) 148–152. doi:10.1016/j.jlumin.2008.09.003

[47] Puchert, M. K., Timbrell, P. Y., & Lamb, R. N. (1996). *Postdeposition annealing of radio frequency magnetron sputtered ZnO films. Journal of Vacuum Science & Technology A: Vacuum,* Surfaces, and Films, 14(4), 2220–2230. doi:10.1116/1.580050

[48] Cotterill, P. and Mould, P. R. (1976). *Recrystallization and Grain Growt in Metals.* Surrey Univ. Press, London. Novikov, V.

[49] Rios, P.R., Siciliano Jr, F., Sandim, H.R.Z., Plaut, R.L., Padilha, A.F., *Nucleation and Growth During Recrystallization,* Materials Research, Vol. 8, (3) (2005) 225-238.

[50] Zahou, L., Wang, S., Ma, H., Ma, S., Xu, D., Guo, Y., *Size-controlled synthesis of copper nanoparticles in supercritical water.* Chemical Engineering Research and Design, 98. (2015) https://doi.org/10.1016/j.cherd.2015.04.004

[51] Voyiadjis, G. Z., Faghihi, D., & Zhang, Y., *A theory for grain boundaries with straingradient plasticity.* International Journal of Solids and Structures, 51(10) (2014)1872–1889. doi:10.1016/ j.ijsolstr .2014.01.02

[52] Ghobadi, N. *Band gap determination using absorption spectrum fitting procedure.* International Nano Letters, 3(1) (2013) doi:10.1186/2228-5326-3-2

[53] Aguirre, J. M., Gutiérrez, A., & Giraldo, O. *Simple route for the synthesis of copper hydroxy salts.* Journal of the Brazilian Chemical Society, 22(3) (2011) 546–551. doi:10.1590/s0103-50532011000 300019

[54] Henrist, C., Traina, K., Hubert, C., Toussaint, G., Rulmont, A., Cloots, R.*, Study of the morphology of copper hydr oxylnitrate nanoplatelets obtained by controlled double jet precipitation and ureahydrolysis*. J. Cryst. Growth. 254 (2003)176-187 https://doi.org/10.1016/S0022-0248(03)01145-X

[55] *Liu, J., Huang, X., Li, Y., Sulieman, K., He, X., Sun, F.*, *Hierarchical nano structures of cupric oxide on a copper substrate: controllable morphology and wettability.* J. Mater. Chem.16 (45) (2006) 4427-4434 https://doi.10.1039/C6DT04500F

[56] Akgul F A, Akgul G, Yildirim, N., Unalan, H. E., Turan, R.*, Influence of thermal annealing on microstructural, morphological, optical properties and surface electronic structure of copper oxide thin films Mater.* Chem. Phys. 147 (2014) 987–995 https://doi.org/10.1016/j.matchemphys.2014.06.047